Chapter 3

Electrochemical sensing of adenine and guanine using a self-assembled copper(II)-thiophenyl-azo-imidazole complex modified gold electrode

3.1. Introduction

Adenine (A) and Guanine (G) are the building blocks of nucleic acids and play an important role in genetic information storage, protein biosynthesis and fulfill a variety of functions in the metabolism of the cell.[1] The abnormal changes of the concentration of A and G in nucleic acid may cause several diseases, including Parkinson's disease, carcinoma and liver diseases.[2] Hence, the determination of A and G has great significance to the bioscience and clinical diagnosis. Various methods have been applied for their detection and measurement, such as chromatography,[3] electrophoresis,[4] chemical luminescence,[5] spectrophotometry [6] or surface enhanced Raman scattering.[7] Although these methods are excellent but have several shortcoming such as high cost, high time consumption and tedious pretreatment steps.

For routine analysis electrochemical techniques are very promising due to low cost, high sensitivity, high selectivity and ease of miniaturization. They are suitable for analysis of A and G individually or simultaneously,[8] still the electrochemical methods suffer problems for the detection of nucleic bases such as slow electron transfer kinetics, high overpotential and overlapping of their oxidation peaks. To overcome the problems, chemical modification of electrode surface with suitable materials is always beneficial. Varieties of materials have been used for the electrode surface modification and used them to electrochemical detection of A and G. Cyclodextrin modified poly(N-acetylaniline) film,[9] graphene oxide intercalated by self-doped polyaniline nanofibers [10] or cobalt(II)phthalocyanine modified carbon paste electrode,[11] porous silicon supported Pt-Pd nanoalloy modified carbon nanotube paste electrode,[12] glassy carbon electrode modified with overoxidized polypyrrole/grapheme,[13] multiwall carbon nanotubes (MWCNTs) decorated with $NiFe_2O_4$ magnetic nanoparticles,[14] silver nanoparticles(AgNPs)–polydopamine(Pdop)@graphene(Gr)composite,[15] single-stranded DNA–poly(sulfosalicylic acid)composite film,[16] TiO_2 nanobelts,[17] graphene-COOH,[18] 1,8,15,22-tetraaminophthalocyanatonickel(II),[19] iron hexacyanoferrate film, azocalixarene,[21] graphine-Nafion composite film,[22] fullerene-C_{60} [23] and gold electrode modified with n-octadecylmercaptan, followed by controllable adsorption of graphene sheets [24] have been used for the electrochemical oxidation and detection of A and G.

However, these modified electrodes have some drawbacks such as stability, reproducibility and use of costly chemicals for electrode modification. In this context, the development of novel, chip and simple strategy for electrode modification is highly desirable. Diazonium salt has been extensively used for the electrode surface modification.[25] Diazonium group functionalized electrode surface can coupled with phenolic, imidazole or amino groups to form different diazotized compounds [26] which are capable of forming metal complexes. There are many reports that metal-azo complexes can interact with the DNA bases and is important in the field of anticancer drug research.[27] A and G formed complexes with metals including copper, has been extensively studied by electrochemical methods.[28] A number of articles have been devoted to the catalytic and electrocatalytic activity of copper(II) modified electrode for the redox reaction of organic and biological compounds. For example, electrocatalytic oxidation of hydroquinone with copper(II)-L-cysteine [29] and copper(II)-5-amino-2-mercaptobenzimidazole [30] complex monolayer modified gold electrode, catalytic oxidation of L-cysteine in oxygen-saturated aqueous solution by copper(II) supported on a polymer,[31] determination of cysteine at a glassy carbon electrode modified by copper(II) ions,[32] determination of ascorbic acid using dinuclear copper salicylaldehyde-glycine schiff base modified GC electrode [33] and copper(II)-zeolite modified electrode,[34] electrocatalytic oxidation of carbohydrates at copper(II) oxide modified electrode [35] and certain catecholamines such as dopamine, L-dopa, epinephrine and norepinephrine using copper(II) complex and AgNPs modified glassy carbon paste electrode.[36]

In the present study, we have used a self-assembled copper(II) containing azoimidazole complex modified gold electrode for the detection of purine bases, A and G, individually and simultaneously in the physiological pH. Electrode modification process and the electrochemical oxidation behaviour of A and G over the modified electrode were studied in detail. The modified electrode has also been applied for the detection of DNA bases in real sample.

3.2. Experimental

3.2.1. Electrode pre-treatment and immobilization of 4-(2′- imidazolylazo)thiophenol over gold electrode

A gold electrode (2 mm in diameter) was polished with 0.05 μm α-alumina on a polishing pad and rinsed extensively with anhydrous ethanol and distilled water. Then the gold electrode was electrochemically cleaned in 0.5 M H_2SO_4 until a steady characteristic gold oxide cyclic voltammogram was obtained.[38] The cleaned gold electrode was immersed into the 4-ATP (1 mM) solution for 20 hours. The self-assembled 4-ATP monolayer was formed over electrode surface via gold-sulfur interaction and the modified electrode was thoroughly washed with ethanol and distilled water. After that the 4-ATP-Au electrode was dipped into a 0.1 M HCl solution at 2 – 4 °C, and 0.1 g $NaNO_2$ solution was added slowly. After 30 minute incubation, the diazotized modified gold electrode (diazo-ATP-Au) was removed and rinsed with ice cold distilled water. For coupling with imidazole, the diazo-ATP-Au electrode was immersed into aqueous 0.025 M imidazole solution for 30 minutes at 2 – 4 °C in stirring condition. Finally, the 4-(2′-imidazolylazo)thiophenol modified gold electrode (IATP-Au) was rinsed with distilled water and dried in air (Fig. 3.1).

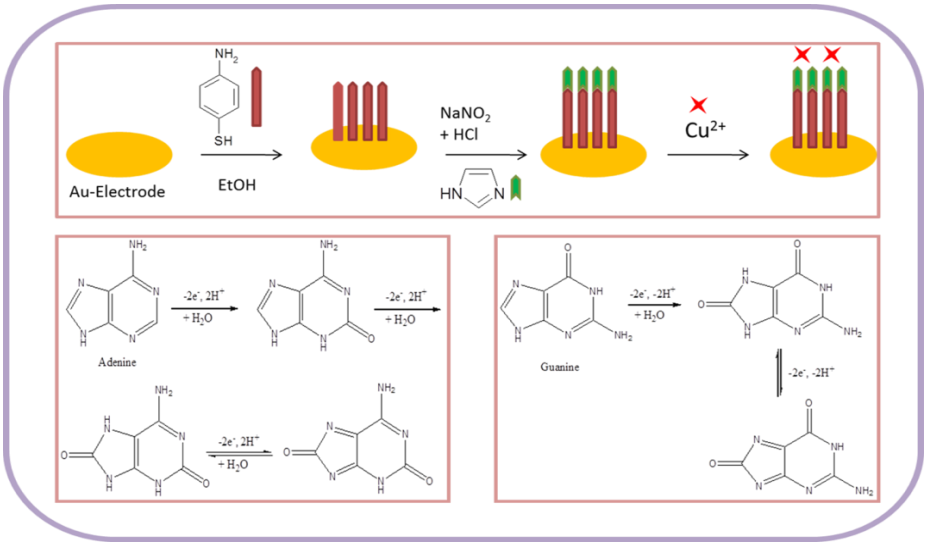

Fig. 3.1. Schematic representation for the fabrication of gold electrode and the electrochemical oxidation mechanism of adenine and guanine.

3.2.2. Copper complexation on IATP/Au electrode

The IATP - Au electrode was immersed into 1×10^{-3} M $CuSO_4$ solution (containing 0.1 M KNO_3) at pH 5.6 and stirred for 4 hours. After complexation, the electrode (Cu^{2+}-IATP-Au) was washed thoroughly with distilled water and then dried in air for further experiment.

3.3. Results and discussion

3.3.1. Choice of Materials

Copper has unique coordination chemistry which renders it suitable for many enzymatic reactions, such as superoxide dismutase (SOD), ascorbic acid oxidase, cytochrome-c-oxidase actions.[39] Imidazole moiety can be found in almost all copper(II) enzymes. In biological system, superoxide dismutase catalyses the dismutation of poisonous superoxide to O_2 and H_2O_2. Copper(II) is the catalytic center in SOD, on reduction by superoxide O_2^-, blue $[Cu^{II}(his^-)(his\text{-}H)_3]$ changes to colourless $[Cu^{I}(his\text{-}H)_4]$. Ascorbic acid oxidase is a blue copper(II) containing protein that catalyses the oxidation of ascorbic acid to dehydroascorbic acid by O_2. Cytochrome-c-oxidase is a terminal enzyme in the respiratory chain. It brings about the oxidation of the reduced form of $[Fe^{II}(Cyt\text{-}c)red]$ with concomitant reduction of molecular oxygen to water. These inspire us to make the biomimetic catalyst containing Cu(II)-Imidazole moiety which can oxidise the purine bases, adenine and guanine and at the same time determine the concentration. Verities of nanomaterials, nano composites and few metal complexes have been used so far for electrode modification and applied for elctrocatalytic oxidation of adenine and guanine.[9-24] Similarly, different copper(II) ion modified electrodes have been used for electrocatalytic oxidation of various organic and biologically important molecules.[29-36] For the first time, we have modified gold electrode by the self-assembled copper(II)-thiophenylazoimidazole complex monolayer and utilized this bio-mimetic sensor for the electrocatalytic oxidation of adenine and guanine in physiological pH. The proposed sensor exhibited a simple, rapid and sensitive determination of adenine and guanine individually as well as simultaneously with low detection limit.

3.3.2. Surface morphology of the Cu^{2+}/IATP modified gold electrode

The step wise modification and surface morphology of the bare and self-assembled monolayer modified gold electrodes were characterized by FE SEM. Fig. 3.2 (A – D) shows the clear change of surface morphology and suggested the formation of Cu^{2+}-IATP film on gold surface.

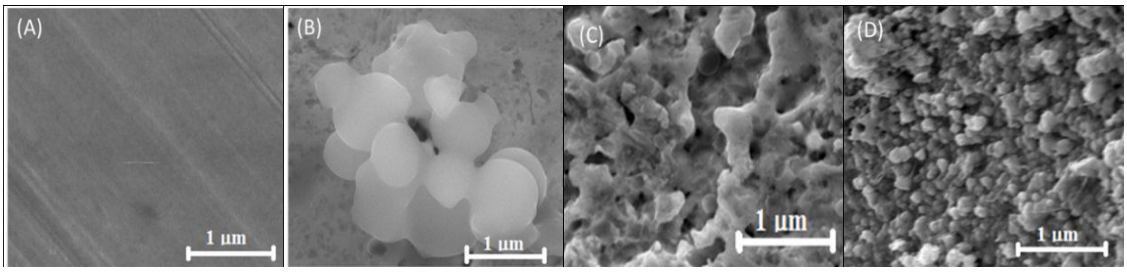

Fig. 3.2. SEM images of bare (A), 4-ATP modified (B), IATP modified (C), Cu^{2+}-IATP modified gold electrode.

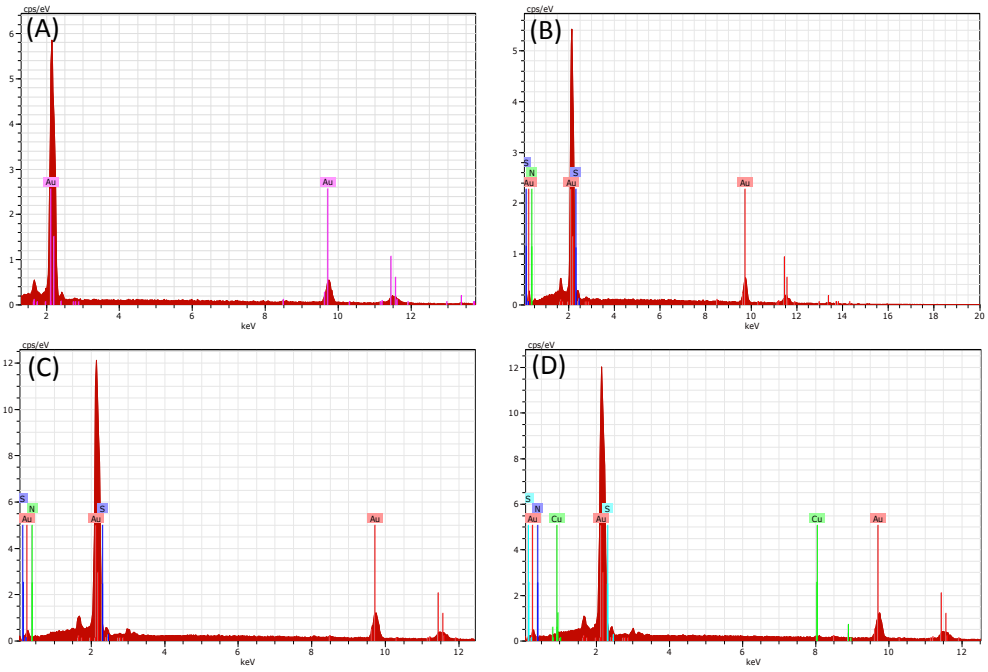

Fig. 3.3. EDAX spectrum of bare (A), 4-ATP modified (B), IATP modified (C), Cu^{2+}-IATP modified gold electrode.

Fig. 3.3 (A -D) is the EDAX images also confirm the step wise modification. In the FTIR spectra (Fig. 3.4), 4-ATP modified gold electrode shows two absorbance peaks at 3443 and 3342 cm^{-1} due to presence of $–NH_2$ group. After diazotization and coupling with imidazole these peaks are absent but a new peak appeared at around 1376 cm^{-1} due to -N=N-bond formation. After complexation with copper(II) ion the –N=N- stretching frequency decreased due to back donation from copper to –N=N- π* orbital and the azo peak observed at 1366 cm^{-1}. Along with these a new peak observed at 460 cm^{-1} and is due to Cu-N bond stretching which also supports the Cu^{2+}- IATP- Au modification.

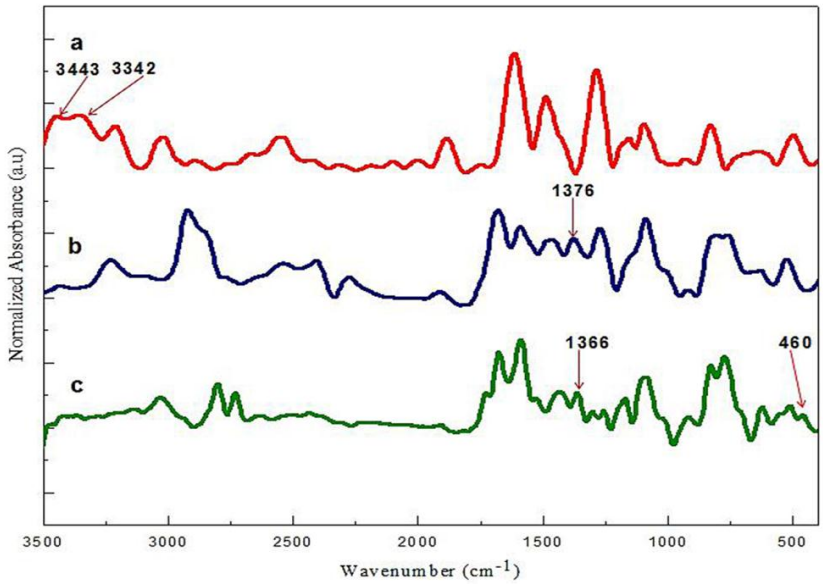

Fig. 3.4. FTIR spectra of (a) 4-ATP modified (b) IATP modified (b) and (c) Cu^{2+}-IATP modified gold electrode.

3.3.3. Electrochemical characterisation of the Cu^{2+}/IATP modified gold electrode

The stepwise modification was examined by CV using $[Fe(CN)_6]^{3-/4-}$ as redox probe in 0.1 M PBS buffer at pH 7 (Fig. 3.5). For the bare electrode the cyclic voltammogram (Fig. 3.5A) of 0.5 mM $[Fe(CN)_6]^{4-}$ exhibit electrochemically reversible redox couple. However, 4-ATP modified Au electrode, the cyclic voltammogram of $[Fe(CN)_6]^{4-}$ exhibit an irreversible feature with low current height than that of bare gold. The current height decreases even more when diazotized (diazo-ATP- Au) and imidazole coupled (IATP - Au) gold electrode was used. The experimental results indicate that the electronic

communication between Au and $[Fe(CN)_6]^{4-}$ is blocked due to SAM formation. Electrochemical impedance spectroscopy supports the CV results. In the Nyquist plot (Fig. 3.5B) the diameter of the semi-circle decreases gradually when step wise modification on the gold electrode surface was carried out. The observed trend is due to the fact that the modified electrode blocked the electron transfer rate for the oxidation of $[Fe(CN)_6]^{4-}$.

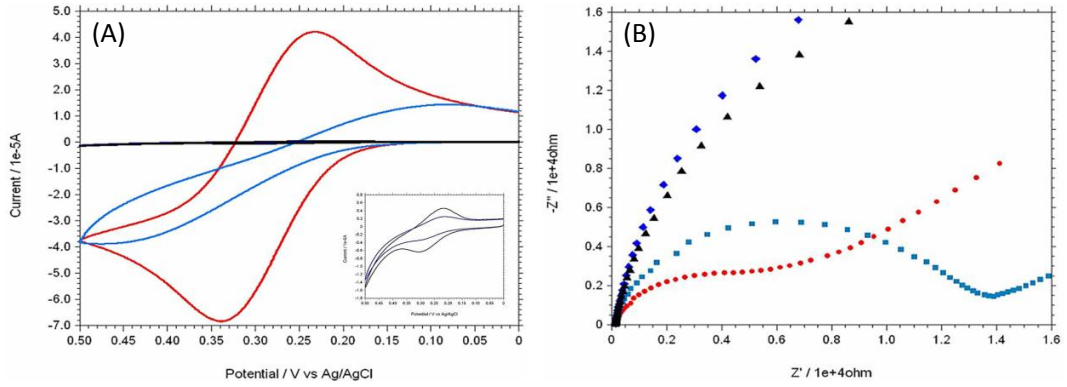

Fig. 3.5. Cyclic voltammograms (A) and Nyquist plot ($-Z^{//}$ versus $Z^{/}$) (B) of 0.5 mM $K_4[Fe(CN)_6]$ in 0.1M PBS at pH 7 using different working electrode [bare Au (red), ATP -Au (light blue), ATP-N^{+2} - Au(dark blue) and IATP - Au (black)]. [Inset: enlarge figure of two overlapping curve for ATP -N^{+2} - Au (dark blue) and IATP - Au (black)]

The IATP - Au can form a neutral monolayer at pH 7. The faradic currents for the probe redox reaction were decrease (Fig. 3.5) when modified the gold electrode surface with IATP. Reasonably, hydrogen bonds have more chance to form between imidazolic NH and π-π staking are more effectively formed in this condition. A value may be obtained for surface coverage $\theta = 0.99$ using $\theta = [1-(i_p/i_p^0)]$ relation [40] where i_p^0 and i_p are peak currents of redox probe at bare and IATP/Au electrodes, respectively under the same condition. The value obtained for i_p^0 and i_p were 3.717×10^{-5} μA and 4.610×10^{-7} μA at pH = 7.0. From EIS spectra the R_{ct} was increased from bare Au ($7.736 \times 10^3\ \Omega$) to IATP - Au ($5.817 \times 10^4\ \Omega$). This difference is due to insulation effects originated from assemblies of neutrally charged IATP layer at pH 7. Assuming that all the current passes through pin-holes and defects, a value may be obtained for θ using $\theta = [1 - (R_{ct}^0 / R_{ct})]$ relation,[40] where R_{ct}^0 and R_{ct} are the charge transfer resistance of redox probe at bare Au

and IATP - Au electrodes under the similar conditions and a value of 0.87 was estimated for θ. The difference observed between θ values obtained from CV and EIS method may be attributed to the contribution of tunnelling effects.[41]

In order to confirm the Cu(II) complexation with azoimidazole on the gold surface (IATP/Au), a comparable CV was taken for bare Au, IATP - Au and Cu^{2+} - IATP - Au in 0.1 M PBS buffer at pH 7 (Fig. 3.6A). A Cu^{2+}/Cu^{+} redox couple ($E_{1/2}$ = 0.3 V, ΔE = 120 mV) supports the formation of Cu^{2+} - IATP - Au SAM.

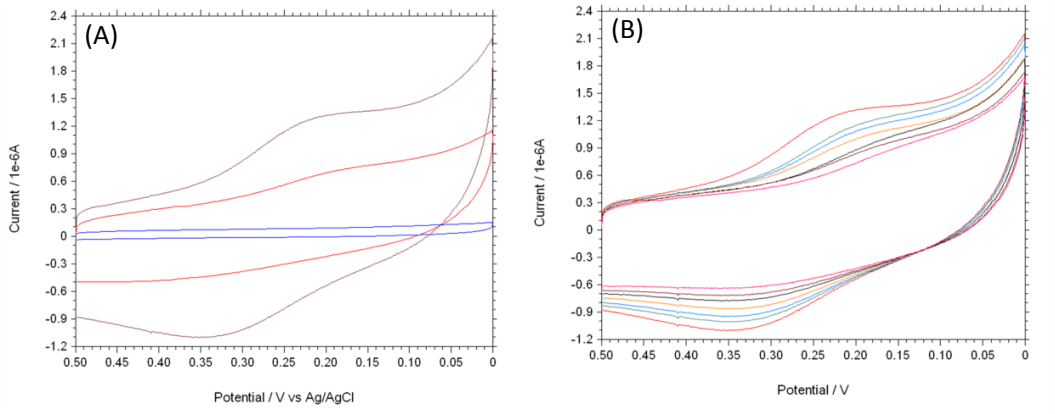

Fig. 3.6. (A) Overlaid cyclic voltammograms of bare Au (red line), ATP-Au (blue line), Cu^{2+}-IATP-Au (violet line) modified electrode and (B) cyclic voltammogram of IATP-Au electrode in varying concentration of $CuSO_4$ [0.1 mM -0.7 mM] in 0.1 M PBS at pH 7.0.

Fig. 3.6B shows the cyclic voltammograms for different concentration (0.1 mM – 0.7 mM) of Cu(II) ion on the IATP - Au modified electrode. Both cathodic and anodic peak current increased with increasing concentration of Cu(II) ions. The influence of pH of the electrolytic solution on the electrochemistry of Cu(II)azo-imidazole complex over Au electrode was studied. The cathodic peak current reached the maximum value at pH 7.0 (Fig. 3.7) which indicates that at this pH strong complexation takes place.

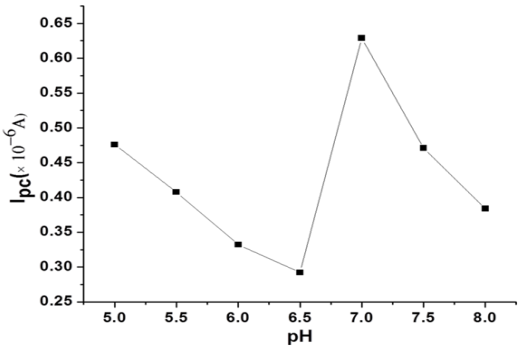

Fig. 3.7. Plot of pH versus cathodic peak current (I_{pc}) for copper complexation with IATP-Au electrode in 0.1 M PBS solution.

Electrochemical impedance spectra of the bare and modified electrodes were taken in 0.1 M PBS buffer at pH 7 and from the Nyquist plot it is clearly shows that the R_{CT} value for Cu^{2+} - IATP - Au electrode is less than IATP - Au or bare Au.

3.3.4. Electrochemical oxidation of adenine and guanine

The modified gold electrode Cu^{2+} - IATP - Au was used for the electrochemical oxidation of nucleobases A and G. Fig. 3.8A shows the cyclic voltammograms of 1 mM guanine in 0.1 M PBS (pH 7) using the bare Au (red curve), IATP - Au (blue curve) and Cu^{2+} - IATP - Au (green curve) electrodes. For bare Au and IATP/Au electrode manifested only a featureless voltammetric profile between 0 to + 1.0 V whereas in case of Cu^{2+} - IATP - Au electrode two irreversible oxidation peaks appeared at + 0.85 V and 0.96 V for guanine. An irreversible oxidation peak was observed at + 1.2 V for adenine when Cu^{2+} - IATP - Au electrode used as working electrode (Fig. 3.8B). No such prominent peak was observed when bare Au (red curve) and IATP/Au (blue curve) electrodes was used under similar condition. The detailed oxidation mechanism of purine bases is shown in Fig. 3.1. Electrochemical oxidation of guanine followed a two-step mechanism with loss of two electrons and two protons in each step and the first step was rate-determining step [42] on the other hand adenine underwent a multistep six electron six protons oxidation involving irreversible chemical steps.[43]

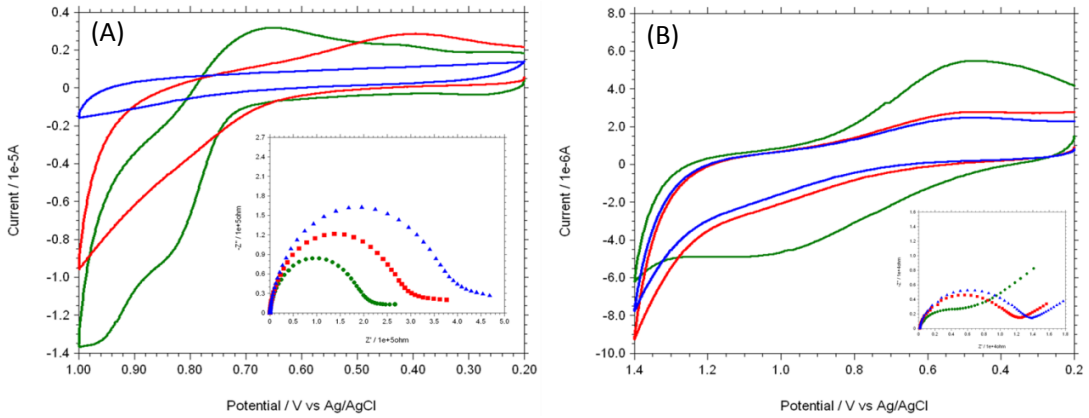

Fig. 3.8. Overlaid cyclic voltammogram and Nyquist plot (inset) of 1 mM Guanine (A) and 1 mM adenine (B) in 0.1 M PBS solution at pH 7 using different working electrodes. [Bare Au (red), IATP - Au (blue) and Cu^{2+} - IATP - Au (green)]

EIS was carried out for both A and G at pH 7.0 (PBS buffer) using the modified and bare electrodes. The diameter of the semicircle observed in the Nyquist plot corresponds to charge transfer resistance, R_{ct}; the smaller the semi-circle, faster is the charge transfer.[44] Fig. 3.8A and 3.8B (inset) shows that the diameter of semi-circle (R_{ct}) changes upon modification of gold electrode surface. The R_{ct} values in different electrode system shows the following tread: IATP-Au (3.9×10^5 Ω) > bare Au (2.9×10^5 Ω) > Cu^{2+}-IATP-Au (1.9×10^5 Ω) and IATP-Au (13.3×10^3 Ω) > bare Au (11.7×10^3 Ω) > Cu^{2+}-IATP-Au (7.2×10^3 Ω) for G and A, respectively. The observed trend is due to the fact that the copper(II) complex modified electrode ease the electron transfer rate for the oxidation of A and G whereas IATP modified gold electrode blocked the electron transfer. Electrochemical impedance measurements clearly indicate that Cu^{2+}-IATP-Au SAM modified electrode has lower resistance as compared to the bare Au and IATP-Au electrodes. This study reveals that the Cu^{2+}-IATP-Au SAM modified electrode is an efficient electrocatalyst for A and G oxidation.

3.3.5. Determination of adenine and guanine using DPV

Based on the optimum conditions, the individual and simultaneous determination of A and G were performed using DPV. Fig. 3.9 and Fig. 3.10 show the DPV curves of G with different concentration.

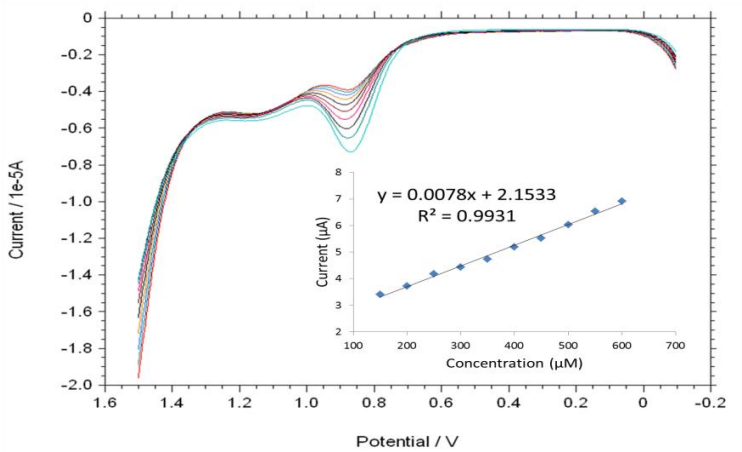

Fig. 3.9. Overlaid DPV with increasing guanine concentration (150 - 600 µM) in 0.1 M PBS (pH 7). [Inset: Plot of current as a function of concentration of guanine with linear trend line ($R^2 > 0.99$)].

In the individual determination of purine bases the oxidation peak current of G was linear with its concentration in the range of 150-600 µM (Inset Fig. 3.9). The detection limit for G is estimated to be 0.007 µM (S/N = 3). Fig. 3.10 indicated that oxidation peak current of A increased linearly in the range of 150 - 600 µM. The detection limit for A was 0.058 µM (S/N = 3).

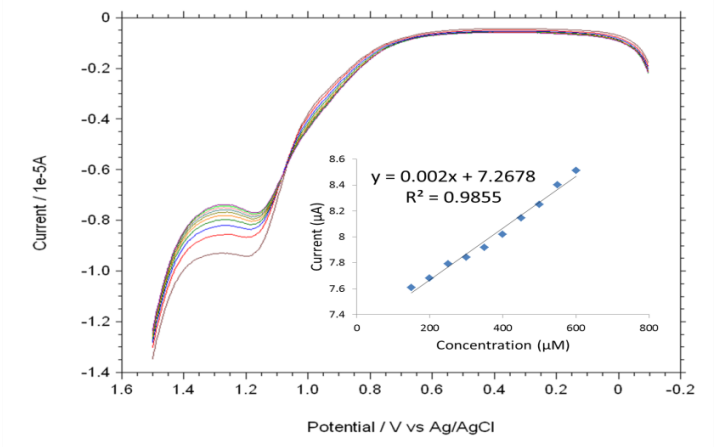

Fig. 3.10. Overlaid DPV with increasing Adenine concentration (150 - 600 µM) in 0.1 M PBS (pH 7). [Inset: Plot of current as a function of concentration of adenine with linear trend line ($R^2 = 0.985$)].

Fig. 3.11 shows the DPV curves of G with different concentrations in the presence of 100 μM A and the oxidation peak current of G was linear with its concentration range of 10 – 60 μM. The regression equation was I_{pa} = 0.0055 c + 1.3113 (R^2 = 0.9917, 95% confidence limit for the slope = ± 0.10 and intercept = ± 0.42) with a detection limit of 0.01 μM (S/N = 3). Similarly, Fig. 3.12 shows the DPV curves of A with different concentrations in the presence of 100 μM G and the oxidation peak current of A increased linearly in the concentration range of 10 – 60 μM. The regression equation was I_{pa} = 0.0088 c + 2.1627 (R^2 = 0.9974, 95% confidence limit for the slope = ± 0.09 and intercept = ±0.31) with a detection limit of 0.06 μM (S/N = 3). For further evaluating the feasibility of the Cu^{2+} - IATP - Au electrode for A and G determination simultaneously by simultaneous changing their concentration (Fig. 3.13).

All the results indicated that the simultaneous and sensitive detection of A and G could be achieved at copper(II) complex modified gold electrode. Table 3.1 shows a comparison of the proposed electrochemical method and the other modified electrodes reported for adenine and guanine. It can be seen that the detection limit and linear range of the proposed method are comparable with the reported methods.

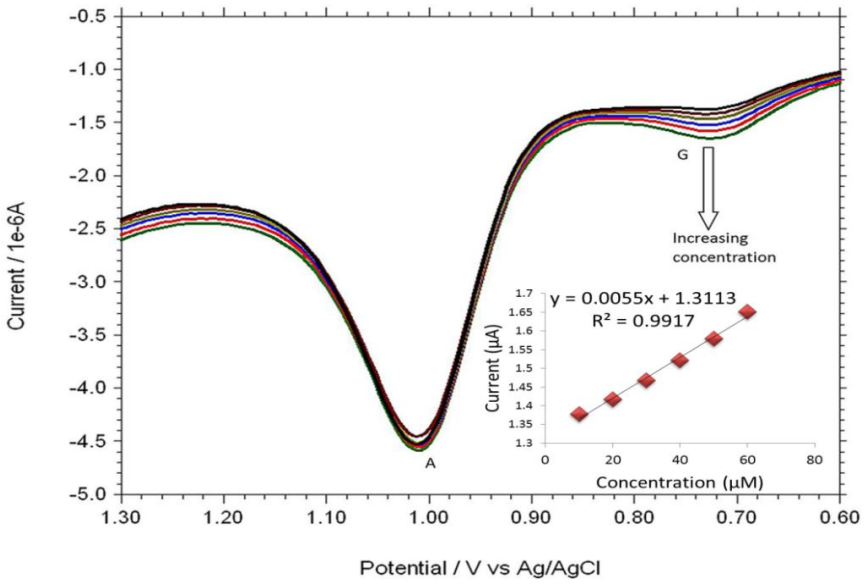

Fig. 3.11. Overlaid DPV for each increment of 10 μM G to 100 μM A at Cu^{2+} - IATP SAM modified gold electrode in 0.1 M PBS buffer solution at pH 7.0.

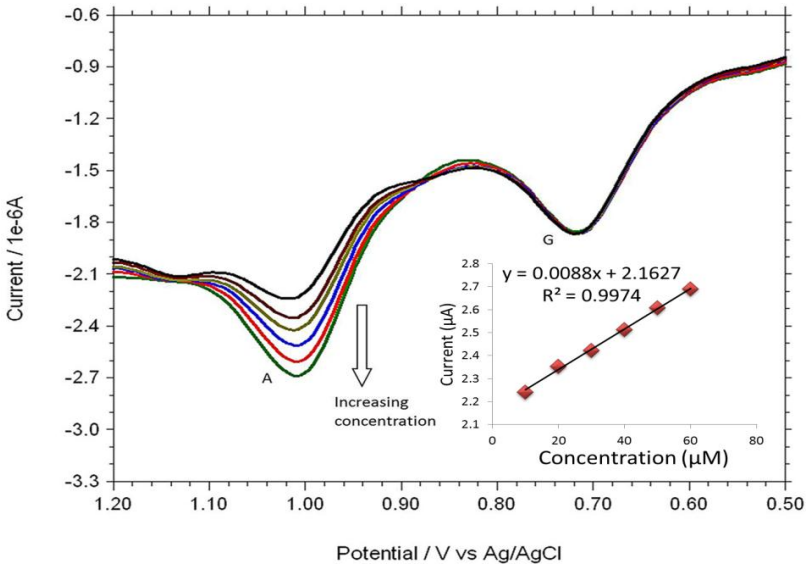

Fig. 3.12. DPVs obtained for each10 µM A to 100 µM G at Cu^{2+} - IATP SAM modified gold electrode in 0.1 M PBS buffer solution at pH 7.0.

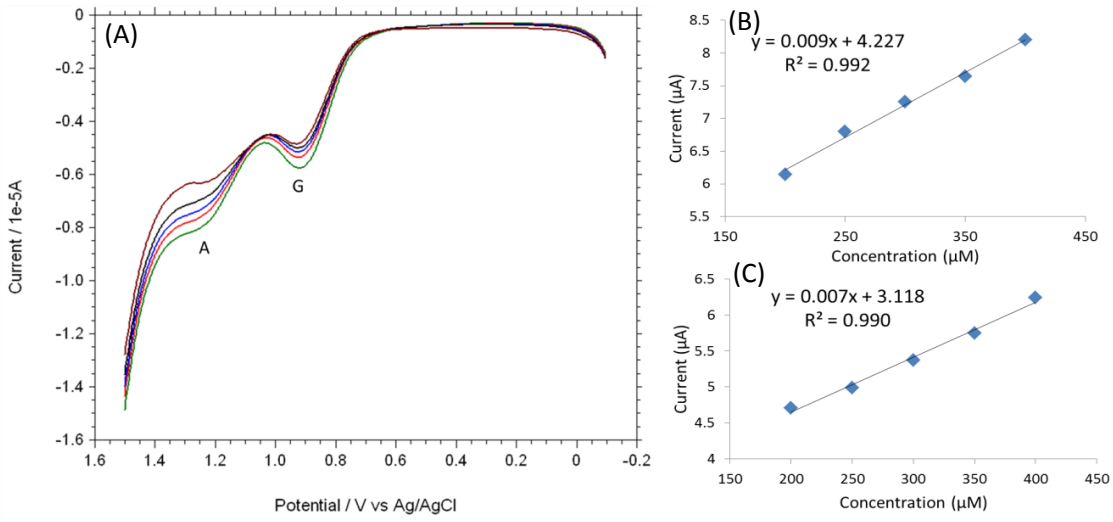

Fig. 3.13. (A) DPV obtained for A and G with each increment of 50 µM each A and G at Cu^{2+}-IATP-Au SAM electrode in 0.1 M PBS (pH = 7). [(B) Plot of current as a function of concentration of adenine with linear trend line (R^2 = 0.992), (C) Plot of current as a function of concentration of guanine with linear trend line (R^2 = 0.99)].

Table 3.1. Comparative account of different electrochemical sensors for the determination of adenine and guanine.

Electrode system	Adenine		Guanine		Ref
	Linear range (μM)	Dete-ction Limit (μM)	Linear range (μM)	Detection Limit (μM)	
GNO–SPAN/CPE	0.5-200	0.05	0.5-200	0.075	10
Pt-Pd/PSi/CNPE	0.1-10	0.03	0.1-10	0.02	12
PPyox/GR/GCE	0.06-100	0.02	0.04-100	0.01	13
MWCNT/$NiFe_2O_4$/GCE	0.1-4.0	0.01	0.05-3.0	0.006	14
AgNPs-Pdop@Gr/GCE	0.02-40	0.002	0.02-40	0.004	15
PSSA–ssDNA /GCE	0.065-1.1	0.02	0.065-1.1	0.02	16
graphene-COOH/GCE	0.5-200	0.025	0.5-200	0.05	18
4α-NiIITAPc/GCE	-	-	10-100	0.03	19
FeHCF/GCE	-	-	0-145	0.10	20
azocalix[4]arene/GCE	0.125-200	0.07	0.125-200	0.05	21
Cu^{2+}/IATP/Au	10 - 60	0.06	10 -60	0.01	This work

3.3.6. Effect of accumulation time and potential

The effect of accumulation time on the oxidation behavior of adenine and guanine at Cu^{2+} - IATP - Au electrode was investigated by DPV.

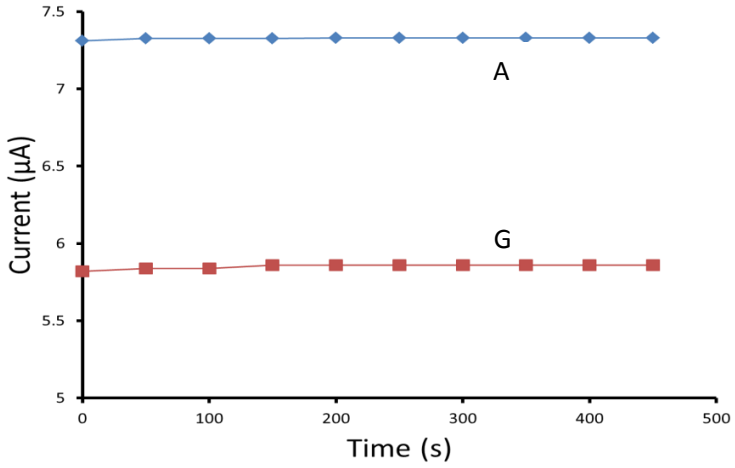

Fig. 3.14. Plot of accumulation time *versus* oxidation peak current for adenine (blue line) and guanine (red line).

Fig. 3.14 shows that both the oxidation peak current of A and G increased slowly with increasing accumulation time from 0 – 150 sec and thereafter they remain constant. Therefore, an accumulation time of 150 sec was chosen as the optimum time for further study. In addition, the influence of accumulation potential on the peak current was examined over the potential range 0.0 to 0.6 V and 0.0 to 0.5 V for adenine and guanine, respectively (Fig. 3.15).

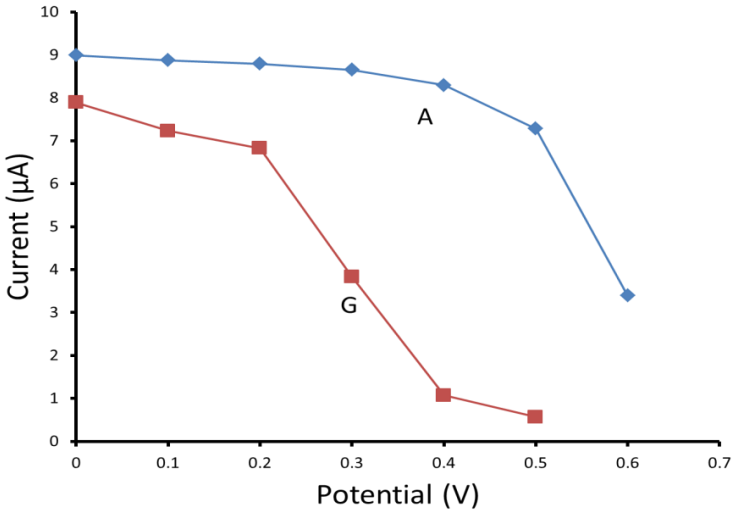

Fig. 3.15 Plot of accumulation potential *versus* oxidation peak current for adenine (blue line) and guanine (red line).

The peak current decreased by changing accumulation potential to more positive value and is due to the oxidation of A and G during the accumulation step at potential higher than 0.6 V and 0.5 V for adenine and guanine, respectively. In fact, the maximum observed currents were equal to those observed for open circuit accumulation.

3.3.7. Effect of scan rate and pH

The oxidation peak current of adenine and guanine increased linearly with the scan rate in the range of 10 - 90 mV/s (Fig. 3.16) following the linear regression equation I_{pa} (μA) = 0.0323 ν (mV s^{-1}) – 0.0624 (R^2 = 0.9939) and I_{pa} (μA) = 0.0393 ν (mV s^{-1}) + 4.7321 (R^2 = 0.9925) for adenine and guanine, respectively. These indicated that the electrooxidation reactions of adenine and guanine at Cu^{2+} - IATP - Au electrode were the surface controlled process.

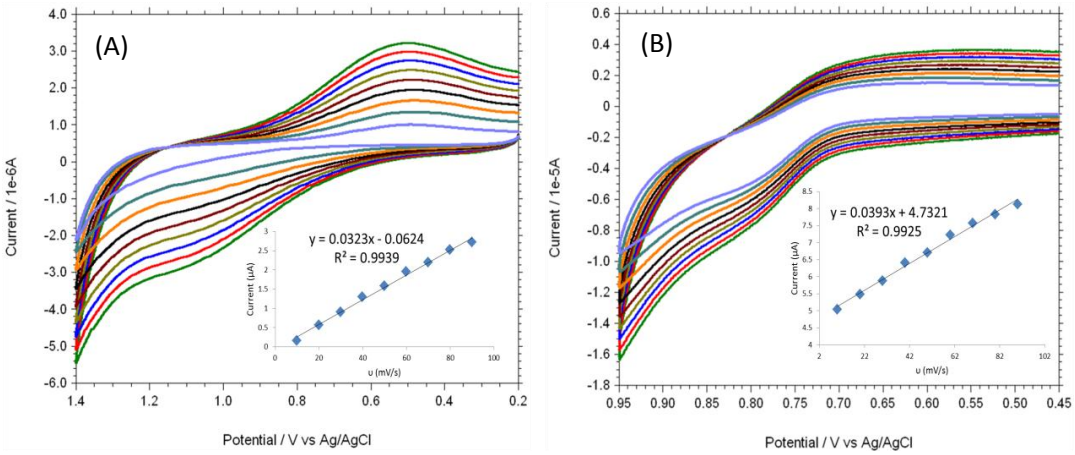

Fig. 3.16. Overlaid cyclic voltammogram of adenine (A) and guanine (B) with different scan rate (10-90 mV/s) at Cu^{2+}-IATP-Au electrode [Inset (A) Plot of current as a function of scan rate of adenine with linear trend line (R^2 = 0.9939) and (B) Plot of current as a function of scan rate of guanine with linear trend line (R^2 = 0.9925).

The effect of pH on the electrooxidation of A and G were also investigated in the range of pH 3.0 – 9.0. As shown in Fig. 3.17 the oxidation peak potential A and G were pH dependent and that they shifted toward more negative potential with increments in solution pH following the linear regression equation of E_{pa} (V) = -0.059 pH + 1.421 (R^2 = 0.994) and E_{pa} (V) = -0.060 pH + 1.169 (R^2 = 0.993), respectively. The slope of 59.0

and 60.0 mV / pH indicated that equal numbers of protons and electrons were involved in the electrode reaction process.[45] Investigation of the influence of pH on the peak current of purine bases at the modified gold electrode revealed that that peak current of A and G reached a maximum at pH 7.0 and then decreased by increasing pH of the solution (Fig. 3.17). On the other hand Cu(II) complexation with azoimidazole on the gold surface (IATP/Au) is maximum at pH 7.0. Considering both results, we have chosen pH 7.0 for the subsequent experiments.

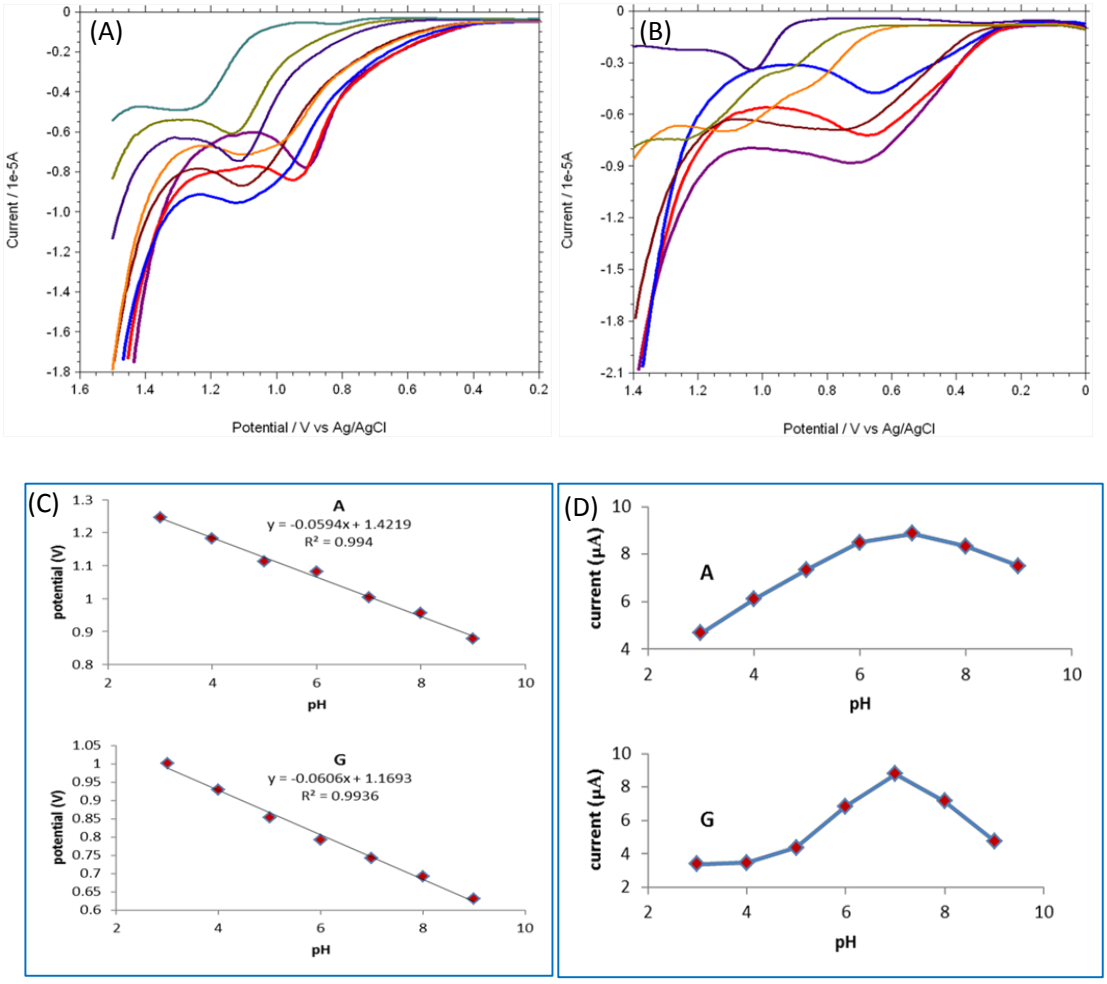

Fig. 3.17. DPV obtained for 1.0 mM adenine (A) and 1.0 mM guanine (B) at Cu^{2+}-IATP-Au electrode in different pH (3.0 – 9.0). (C) The Plot of the oxidation peak potential *versus* the solution pH for A and G. (D) The Plot of the oxidation peak current *versus* the solution pH for A and G.

3.3.8. Interference, reproducibility and stability

The current responses of A and G were studied in presence of some common electroactive interferences such as ascorbic acid, citric acid, cysteine, glucose, Na^+, K^+, Cl^- and SO_4^{2-} in 0.1 M PBS. A 1000 fold excess of ascorbic acid, citric acid, cysteine, glucose, Na^+, K^+, Cl^- and SO_4^{2-} had no effect on the peak currents of the A and G. A representative DPV is given in Fig. 3.18 where ascorbic acid was used 1000 fold excess in A and G mixture.

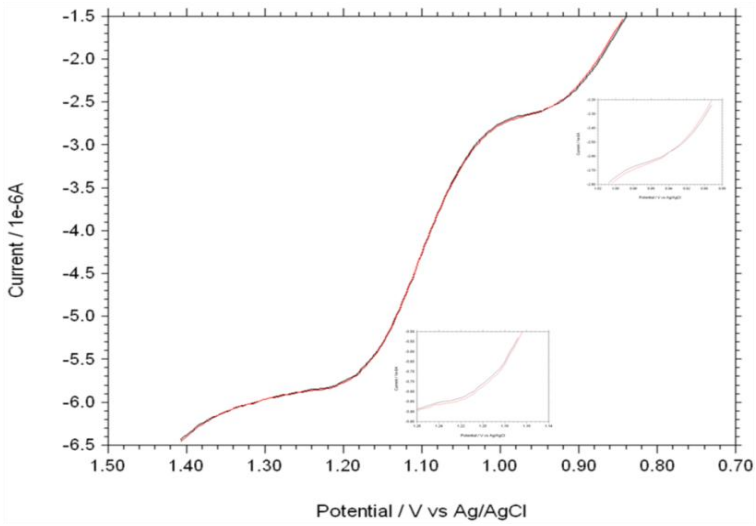

Fig. 3.18. DPV of A and G in presence of 1000 fold excess of Ascorbic acid.

The modified electrode shows reproducible results for A and G. The reproducibility of the modified electrode was examined by 8 successive DPV measurements of A and G in PBS solution. The results showed a relative standard deviation (RSD) of 0.5 %, indicating that the electrode has good reproducibility. The modified electrode also displays good storage stability if kept in aqueous medium at room temperature over a period of 30 days. The modified electrode shows reproducible results for A and G. The reproducibility of the modified electrode was examined by 8 successive DPV measurements of A and G in PBS solution. The results showed a relative standard deviation (RSD) of 0.5 %, indicating that the electrode has good reproducibility. The modified electrode also displays good storage stability if kept in aqueous medium at room temperature over a period of 30 days.

3.3.9. Real sample analysis

The copper (II) complex modified gold electrode, Cu^{2+} - IATP – Au, was used to determine DNA bases simultaneously in the denatured herring sperm DNA sample. Fig. 3.19 shows the overlaid DPV of PBS, herring sperm DNA solution and after addition of standard A, G solution in herring sperm DNA solution. The DPV of herring sperm DNA clearly shows four oxidation peaks for four DNA bases. The content of A and G in herring sperm DNA were calculated using the standard addition method and direct interpolation of the linear regression. The results are summarised in Table 3.2 and agree with the data reported in literature.[21] The accuracy of the method was also verified by recovery studies adding standard DNA base solution to the real sample and 99-100 % recoveries were obtained.

Table 3.2. Determination of A and G in herring sperm DNA sample with copper(II) complex modified gold electrode.

Bases	Detected (μM)	Added (mM)	Found (mM)	Recovery (%)
A	4.4 ± 0.04	1.0	0.99	99.0
G	3.5 ± 0.01	1.0	1.004	100.4

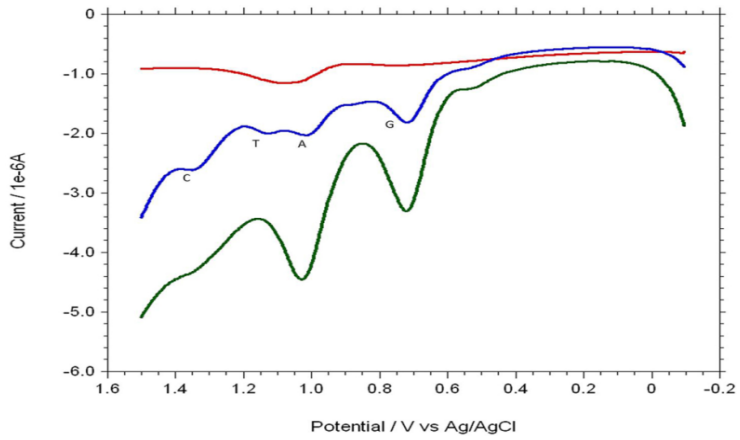

Fig. 3.19. Overlaid DPVs of 0.1 M PBS solution (red), herring sperm DNA solution (blue) and after addition of standard A, G solution in herring sperm DNA solution (green).

3.4. Conclusions

A novel electrochemical sensor has been prepared and is used to detect A and G individually, simultaneously in a mixture and in herring sperm DNA. The electrochemical oxidation of A and G was studied using cyclic voltammetry and a prominent anodic oxidation peak was observed using Cu^{2+} - IATP - Au modified electrode. EIS results show the following order of charge transfer resistance: IATP - Au > bare Au > Cu^{2+} -IATP - Au for A and G in PBS (pH 7) and supports the electrocatalytic nature of copper complex modified gold electrode. Distinguishable oxidation peaks of the A and G can be obtained using Cu^{2+} - IATP - Au modified electrode which is very helpful to analyse DNA fragments simultaneously. The modified electrode showed high sensitivity, low detection limit, higher reproducibility and good stability. Moreover, the electrode modification process is easy, economic as well as reproducible. The new sensor can be used for clinical diagnosis and genetic research.

3.5. References

1. W. Saenger in: C. R. Cantor (Ed.), *Principles of Nuclic acid structure*, Springer, New York, 1984; E. Palecek, Electrochemical behaviour of biological macromolecules, *Bio-electrochem. Bioenerg*., 1986, **15**, 275.

2. H. S. Wang, H.X. Ju and H. Y. Chen, *Anal. Chim. Acta*, 2002, **461**, 243; P. Cekan and S. T. Sigurdsson, *J. Am. Chem. Soc*., 2009, **131**, 18054.

3. C. C. Carrion, S. Armenta, B. M. Simonet, M. Valcarcel and B. Lendl, *Anal. Chem*., 2011, **83**, 9391.

4. C. W. Klampfl, M. Himmelsbach, W. Buchberger and H. Klein, *Anal. Chim. Acta*, 2002, **454**, 185; W. R. Jin, H. Y. Wei and X. Zhao, *Electroanalysis*, 1997, **9**, 770.

5. E. B. Liu and B. C. Xue, *J. Pharm. Biomed.*, 2006, **41**, 649.

6. I. Heisler, J. Keller, R. Tauber, M. Sutherland and H. Fuchs, *Anal. Biochem*., 2002, **302**, 114.

7. M. Ishikawa, Y. Maruyam, J. Y. Ye and M. Futamata, *Journal of Luminescence*, 2002, **98**, 81.

8. X. H. Cai, B. Ogorevc and K. Kalcher, *Electroanalysis*, 1995, **7**, 1126; K. J. Ituang, D. J. Niu, J. Y. Sun, C. H. Han, Z. W. Wu, Y. L. Li and X. Q. Xiong, *Colloids and Surfaces B: Biointerfaces*, 2011, **82**, 543; J. –M. Zen, M. –R. Chang and G. Ilangovan, *Analyst*, 1999, **124**, 679.

9. A. Abbaspour and A. Noori, *Analyst*, 2008, **133**, 1664.

10. T. Yang, Q. Guan, Q. Li, L. Meng, L.Wang, C. Liu and K. Jiao, *J. Mater. Chem. B*, 2013, **1**, 2926.

11. A. Abbaspour, M. A. Mehrgardi and R. Kia, *J. Electroanal. Chem*., 2004, **568**, 261.

12. A. A. Ensafi, M. M. Abarghoui and B. Rezaei, *Sens. Actuators B*, 2014, **204**, 528.

13. Y-S. Gao, J-K. Xu, L-M. Lu, L-P. Wu, K-X. Zhang, T. Nie, X-F. Zhu and Y. Wu, *Biosens. Bioelectron.*, 2014, **62**, 261.

14. A. A. Ensafi, M. J-Asl, B. Rezaei and A. R. Allafchian, *Sens. Actuators B*, 2013, **177**, 634.

15. K-J. Huang , L. Wang, H-B. Wang, T. Gan, Y-Y. Wu, J. Li and Y-M. Liu, *Talanta*, 2013, **114**, 43.

16. L. J. Feng, X.-H. Zhang, P. Liu, H. –Y. Xiong and S. –F. Wang, *Anal. Biochem*., 2011, **419**, 71.

17. J. Cui, D. Sun, W. Zhou, H. Liu. P. Hu, N. Ren, H. Qin, Z. Huang, J. Lin and H. Ma, *Phys. Chem. Chem.. Phys*., 2011, **13**, 9232.

18. K. –J. Huang, D. –J. Niu, J. –Y. Sun, C. –H. Han, Z. –W. Wu, Y. –L. Li and X. –Q. Xiong, *Colloids and Surfaces B: Biointerfaces*, 2011, **82**, 543.

19. A. J. Jeevagan and S. A. John, *Anal. Biochem.*, 2012, **424**, 21.

20. S. M. Chen, C. –H, Wang and K. –C.Lin, *Int. J. Electrochem. Sci*., 2012, **7**, 405.

21. Q. Xu, X. Liu, H. Li, L. Yin and X. Hu, *Biosens. Bioelectron*., 2013, **42**, 355.

22. H. Yin, Y. Zhou, Q. Ma, S. Ai, P. Ju, L. Zhu and L. Lu, *Process. Biochem.*, 2010, **45**, 1707.

23. R. N. Goyal, V. K. Gupta, M. Oyama and N. Bachheti, *Talanta*, 2007, **71**, 1110.

24. X. Xie, K. Zhao, X. Xu, W. Zhao, S. Liu, Z. Zhu, M. Li, Z. Shi and Y. Shao, *J. Phys. Chem. C*, 2010, **114**, 14243.

25. E.Radi, X. M. Berbel, M. C. Puig and J. L. Martyc, *Electroanalysis*, 2009, **21**, 696; L.S. Jiao, L. Niu, J. Shen, T. Y. You, S. J. Dong and A. Ivaska, *Electrochem. Commun.*, 2005, **7**, 219.

26. G. T. Hermenson, 2008, *Bioconjugate Techniques*, 2nd Ed. Academic Press, San Diego, CA; F. Li, Y. Feng, P. Dong, B. Tang, *Biosens. Bioelectron.*, 2010, **25**, 2084.

27. Sk. Jasimuddin, *Trans. Met. Chem*., 2006, **31**, 724; Sk. Jasimuddin and C. Sinha, *Trans. Met. Chem.*, 2004, **29**, 566.

28. L. Trnkova, L. Zerzankova, F. Dycka, R. Mikelova and F. Jelen, *Sensors*, 2008, **8**, 429.

29. K. Barman and Sk. Jasimuddin, *Indian J. Chem., Sec. A*, 2013, **52A**, 217.

30. R. K. Shervedani, F. Yaghoobi, A. H. Mehrjardi and S. M. S. Barzoki, *Electrochim. Acta*, 2008, **53**, 4185.

31. S Y M Shikov, A. V. Vurasko, L. S. Molechmikov, E. G. Kovalyova and A. A. Ffendieu, *J. Mol. Catal. A Chem.*, 2000, **158**, 447.

32. Z. Dursun, I. Sahbaz, F. N. Ertas and G. Nisli, *Turkish J. Chem.*, 2003, **27**, 513.

33. Z. Zhang, X. Li, C. Wang, C. Zhang, P. Liu, T. Fang, Y. Xiong and W. Xu, *Dalton Trans.*, 2012, **41**, 1252.

34. T. Rohani and M. A. Taher, *Talanta*, 2009, **78**, 743.

35. K. Kano, M. Torimura, Y. Esaka, M. Goto, *J. Electroanal. Chem*., 1994, **372**, 137.

36. B. J. Sanghavi, S. M. Mobin, P. Mathur, G. K. Lahiri and A. K. Srivastava, *Biosens. Bioelectron.*, 2013, **39**, 124.

37. J. F. Smalley, K. Chalfant, S. W. Feldberg, T. M. Nahir and E. F. Bowden, *J Phys. Chem. B*, 1999, **103**, 1676.

38. R. K. Shervedani, A. Hatefi-Mehrjardi and M. KhosraviBabadi, *Electrochem. Acta*, 2007, **52**, 7051 and references therein.

39. G. G. Hammes, *Enzyme catalysis and regulation*, Academic: New York, 1982; T. Palmer, *Understanding Enzymes*, 2nd Ed. Ellis. Horwood: Chicester, 1985; G. N. Mukherjee and A. Das, *Elements of Bioinorganic Chemistry*, 1st Ed. 1993, U. N. Dhur & Sons Pvt. Ltd., Kolkata.

40. R. K. Shervedani, S. M. S-Barzoki and M. Bagherzadeh, *Electroanalysis*, 2010, **22**, 969.

41. S. Campuzano, M. Pedrero, C. Montemayor, E. Fatas and J. M. Pingarron, *J. Electroanal. Chem*., 2006, **586**, 112.

42. Q. Li, C. Batchelor-McAuley and R. G. Compton, *J. Phys. Chem. B*, 2010, **114**, 7423; L M. Goncalves, C. Batchelor-McAuley, A. A. Barros and R. G. Compton, *J. Phys. Chem. C*, 2010, **114**, 14213.

43. Y. Wei, Q. A. Huang, M. G. Li, X. J. Huang, B. Fang and L. Wang, *Electrochim. Acta*, 2011, **56**, 8571.

44. P. N. Mashazi, P. Westbroek, K. I. Ozoemena and T. Nyokong, *Electrochim. Acta*, 2007, **53**, 1858.

45. E. Laviron, *J. Electroanal. Chem*., 1974, **52**, 355.